 

# Synthesis and Catalysis of Polymer-Protected Pd/Ag/Rh Trimetallic Nanoparticles with a Core–Shell Structure

**Toru Matsushita,[1] Yukihide Shiraishi,[2,3] Shin Horiuchi,[4] and Naoki Toshima*[2,3]**

[1]Graduate School of Science and Engineering, Tokyo University of Science, Yamaguchi, SanyoOnoda 756-0884

[2]Department of Materials Science and Environmental Engineering, Tokyo University of Science, Yamaguchi, SanyoOnoda 756-0884

[3]Advanced Materials Institute, Tokyo University of Science, Yamaguchi, SanyoOnoda 756-0884

[4]Nanoscientific Measurements Group, Nanotechnology Research Institute, National Institute of Advanced Industrial Science and Technology (AIST), Tsukuba Central 4, 1-1-1 Higashi, Tsukuba 305-8562

Received November 14, 2006; E-mail: toshima@ed.yama.tus.ac.jp

Colloidal dispersions of polymer-protected Pd/Ag/Rh trimetallic nanoparticles were synthesized via self-organization by mixing colloidal dispersions of polymer-protected Rh nanoparticles with those of polymer-protected Pd/Ag bimetallic nanoparticles with a core–shell (Pd-core/Ag-shell) structure, which were prepared in advance by a sacrificial hydrogen-reduction method. The Pd/Ag/Rh trimetallic nanoparticles appeared to have a triple core–shell (Pd-core/Ag-interlayer/Rh-shell) structure on the basis of UV–vis absorption spectra, FT-IR spectra of adsorbed CO, TEM, HR-TEM, and EF-TEM observation. The spontaneously formed trimetallic nanoparticles having an atomic composition of Pd/Ag/Rh = 1/2/13.5 and an average diameter of 2.2 nm showed the highest catalytic activity among the metal nanoparticle catalysts tested here for hydrogenation of methyl acrylate at 30 °C under atmosphere of hydrogen.

Metal nanoparticles, nanoscopic metal particles, or fine particles of metal in a nanometer size have received much attention recently, because they have specific chemical and physical properties much different from those of bulk metal.[1,2] They are expected to be useful in various ways, like as catalysts,[3–7] magnetic materials,[8–11] semiconductors,[12,13] electro-optic materials,[14,15] drug delivery materials,[16] and so on, and thus should be attractive to many researchers.

Among these applications, their use as catalysts has been most commonly investigated by many researchers, because the metal nanoparticle catalysts are much different from practical heterogeneous and homogeneous ones. The peculiar catalytic properties of metal nanoparticles are considered to be attributed to their high specific surface area and special surface structure. The polymer-protected metal nanoparticles can be used as colloidal dispersions in solution and as solids supported on inorganic supports in gas phase. From the viewpoint of catalyst design,[3–7] it is of great importance to develop metal catalysts arranged on the nanometer scale in order to provide superior functions to metal nanoparticles with uniform size and narrow size distribution.

Bimetallic nanoparticles, which are composed of two metal elements in a particle, often have higher catalytic activity and/or selectivity than the monometallic ones. In this case, the catalytic activity depends not only on the composition but also on the structure of bimetallic nanoparticles. Among various structures of bimetallic nanoparticles, the most interesting one could be a core–shell structure, in which one element forms a core and the other element covers the core to form a shell.[17]

We have already reported the formation of core–shell-structured bimetallic nanoparticles by simultaneous reduction,[17–19] sacrificial hydrogen reduction,[20] and self-organization by mixing two colloidal dispersions in solution at room temperature.[21,22] In the core–shell-structured bimetallic nanoparticles thus prepared, the catalytic activity of shell atoms can be electronically affected by the core atoms.[23] Based on the concept of electronic effect in bimetallic nanoparticles having a core–shell structure, a "triple core–shell structure," in which one element form a core, the second element covers the core, forming an interlayer, and the third element covers the interlayer, forming a shell, has been proposed. A successive electronic effect is expected in this triple core–shell-structured trimetallic nanoparticle. However, only few reports have been published on trimetallic nanoparticles having a triple core–shell structure. Henglein has reported the formation of Pd-core/Au-interlayer/Ag-shell trimetallic nanoparticles by successive reduction of the corresponding metal ions with $\gamma$-irradiation,[24] although they have not been applied to catalysis.

We have briefly reported on the formation of the present Pd/Ag/Rh trimetallic nanoparticles in a previous paper.[25] Here, we describe the syntheses and characterization of Pd/Ag bimetallic and Pd/Ag/Rh trimetallic nanoparticles, as well as their catalytic activities towards hydrogenation of olefin. Interestingly, the catalytic activity strongly depended on the composition. Only the trimetallic nanoparticles with strictly designed composition had very high activity, which suggests that the triple core–shell structure was spontaneously produced at the specific composition.

Published on the web June 13, 2007; doi:10.1246/bcsj.80.1217

## Experimental

**Chemicals.** Ethylene glycol by Nacalai Tesque, Inc., palladium(II) acetate and silver perchlorate from Kojima Chemicals Co., Ltd., rhodium(III) nitrate from Junsei Chemical Co., Ltd., and palladium(II) chloride, rhodium(III) chloride, 1,4-dioxane, sodium hydroxide, ethanol, and poly(*N*-vinyl-2-pyrrolidone) (PVP, K-30, average molecular weight 40000) from Wako Pure Chemical Industries, Ltd. were used without further purification. Methyl acrylate from Wako Pure Chemical Industries, Ltd. was used as a substrate for hydrogenation after further purification by vacuum distillation.

**Preparation of Rh Nanoparticles.** A 100-mL solution of $RhCl_3$ (rhodium(III) chloride, 0.66 mM) in a 1/9 (v/v) mixed solvent of water and ethanol in a two-necked 200-mL flask was refluxed for 2 h under nitrogen in the presence of poly(*N*-vinyl-2-pyrrolidone) (PVP, average molecular weight 40000, 0.293 g, 2.63 mmol as monomeric residue, *R* (molar ratio of monomeric residue to metal) = 40) as protecting polymer. PVP-protected Rh nanoparticles thus prepared were collected by filtration with an ultrafilter (Advantec, Q0100076E, cut off molecular weight = 10000) and washed with ethanol to remove byproducts under nitrogen, and then were dried under vacuum at 40 °C. The dried metal nanoparticles were dispersed in a 1/1 (v/v) mixed solvent of ethanol and water to give a Rh concentration of 0.66 mM.

**Preparation of Pd-Core/Ag-Shell Bimetallic Nanoparticles.** A typical procedure to prepare polymer-protected Pd-core/Ag-shell bimetllic nanoparticles is as follows: PVP (26.4 mmol in monomeric residue) and palladium(II) acetate (49.4 mg, 0.22 mmol) in dioxane (20 mL) were dissolved in ethylene glycol (100 mL) in a three-necked 500-mL flask. The pH of the mixture was adjusted to 8 by adding aqueous NaOH (0.1 M) while stirring. The colloidal solution of Pd hydroxide and PVP in ethylene glycol was stirred at 160 °C for 3 h with a nitrogen flow passing through the reaction system to prepare Pd nanoparticles. The PVP-protected Pd nanoparticles in glycol were collected by filtration with an ultrafilter and washed with ethanol to remove the byproducts under nitrogen, and then dried under vacuum at 40 °C. The Pd nanoparticles thus prepared were used as core seeds for preparation of Pd-core/Ag-shell-structured bimetallic nanoparticles.

The seed Pd nanoparticles were dispersed into 1/1/1 (v/v/v) mixture of water, ethylene glycol, and ethanol (150 mL) in a three-necked 500-mL flask equipped with a dropping funnel, which was charged with a degassed aqueous solution (100 mL) of silver perchlorate (91.2 mg, 0.44 mmol). The reaction flask was connected with a hydrogen balloon as well. Air in the reaction flask was first replaced with hydrogen, and the seed Pd nanoparticles dispersed in the flask were treated with hydrogen while stirring for 2 h. The silver perchlorate solution was added into the reaction mixture dropwise over about 12 h period. And the reaction was continued for another 12 h under hydrogen at room temperature. The PVP-protected Pd-core/Ag-shell bimetallic nanoparticles thus produced were collected on an ultrafilter, washed with ethanol, and dried under vacuum at 40 °C. The dried metal nanoparticles were dispersed in a 1/1 (v/v) mixture of ethanol and water to give a total metal concentration (Pd + Ag) of 0.66 mM.

**Preparation of Pd-Core/Ag-Interlayer/Rh-Shell Trimetallic Nanoparticles.** The PVP-protected Pd-core/Ag-interlayer/Rh-shell trimetallic nanoparticles with designed compositions were prepared by mixing the colloidal dispersion of PVP-protected Pd-core/Ag-shell bimetallic nanoparticles with the colloidal dispersion of PVP-protected Rh monometallic nanoparticles in the required atomic ratios at room temperature.

**Characterization.** Ultraviolet and visible (UV–vis) spectra were obtained at room temperature using a Shimadzu 2500PC recording spectrophotometer equipped with a 10 mm quartz cell. Transmission electron microscopy (TEM) and high-resolution TEM, performed with a JEOL JEM-1230 electron microscope, operated at 80 kV and a JEOL JEM-2010F electron microscope operated at 200 kV, respectively, were used to characterize the monometallic, bimetallic, and trimetallic nanoparticles. Elemental analysis of one nanoparticle was performed with a NORAN-UTV energy-dispersive spectrometer (EDS) attached to the HR-TEM equipment. Samples for TEM and HR-TEM were prepared by placing a drop of the colloidal dispersion of nanoparticles onto a carbon-coated copper microgrid, followed by evaporation of the solvent. An average diameter was calculated by counting the diameters of 200 particles with a magnifier (10 times) on the TEM photograph at a magnification of 100000. Energy-filtered TEM (EF-TEM) was measured by using a Carl Zeiss LEO912 electron microscope operated at 200 kV to map the distribution of elements by sorting out a specific atom in the spectrum obtained from electron energy loss spectroscopy (EELS). Detailed analyses of Pd-core/Ag-shell bimetallic and Pd-core/Ag-interlayer/Rh-shell trimetallic nanoparticles were performed by using EF-TEM with samples that were prepared by a method similar to that for TEM measurement. In other words, a drop of the colloidal dispersion of nanoparticles was placed onto a carbon-coated copper microgrid or an osmium microgrid, which was specially prepared just before the observation. For measuring the adsorbed CO by Fourier-transformed infrared (FT-IR) spectroscopy, a dispersed solution of metal nanoparticles in dichloromethane was degassed by three freeze–thaw cycles, and filled with 1 atm of CO. FT-IR spectra were obtained on a JEOL JIR-Winspec 50 FT-IR spectrophotometer at room temperature.

The catalytic activities of bimetallic and trimetallic nanoparticles were evaluated by the rate of hydrogenation of methyl acrylate. Ethanol dispersions of bimetallic and trimetallic nanoparticles (0.3 mL, $2.0 \times 10^{-4}$ mmol of total metal) and ethanol (18.7 mL) were placed in a flask, the atmosphere of which was replaced in advance with 1 atm of hydrogen. The mixtures were kept at 30 °C for 2 h while stirring to activate the catalyst. Then, an ethanol solution (1 mL) containing methyl acrylate (43.0 mg, 0.5 mmol) was added to the mixture keeping the total pressure at 1 atm. The reaction was followed by hydrogen uptake, using the initial slope from which the catalytic activity was determined. In order to achieve enough accuracy, we carried out the hydrogenation reaction 8 times under the same conditions and used an averaged value of the catalytic activity.

## Results and Discussion

**Pd/Ag Bimetallic Nanoparticles.** Colloidal dispersions of PVP-protected Pd/Ag bimetallic nanoparticles with a Pd-core/Ag-shell structure were prepared by a so-called "sacrificial hydrogen reduction" method.[20] Polymer-protected Pd nanoparticles, prepared separately from palladium(II) acetate by an alcohol reduction method in ethylene glycol (average diameter = 4.4 ± 1.2 nm), were treated with hydrogen in advance, and then a solution of silver perchlorate was slowly added to the colloidal dispersion of hydrogen-treated seed Pd nanoparticles. No aggregates or precipitates were observed in the colloidal dispersions of PVP-protected Pd/Ag bimetallic nanoparticles thus prepared. The bimetallic nanoparticles were

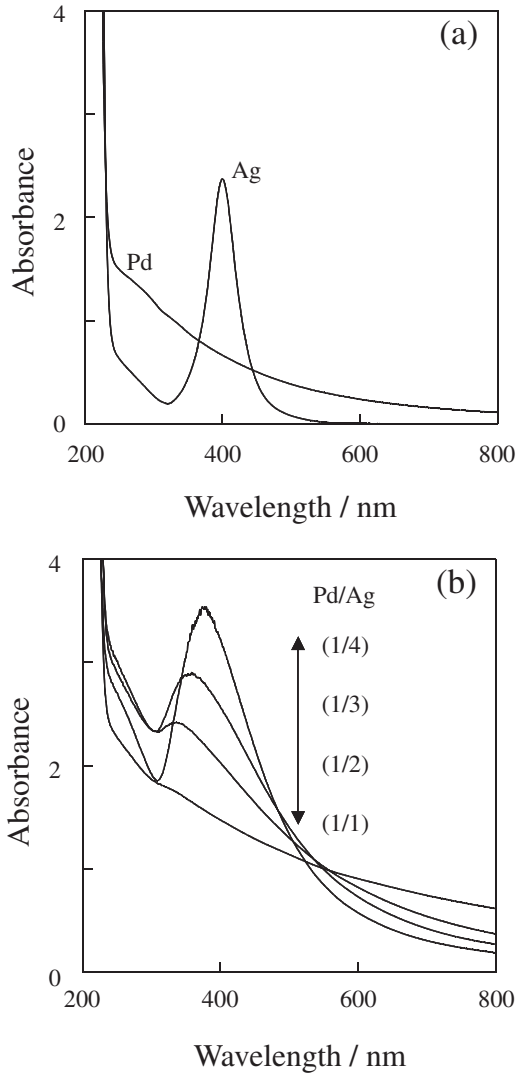


Fig. 1. UV–vis spectra of the dispersions of (a) PVP-protected Pd and Ag monometallic nanoparticles, and (b) PVP-protected Pd/Ag bimetallic nanoparticles at the atomic ratio Pd/Ag = 1/4, 1/3, 1/2, and 1/1.

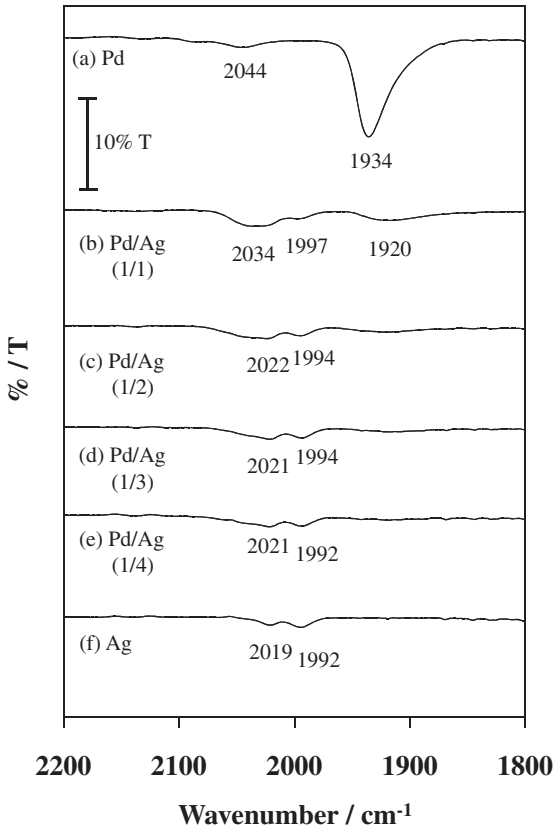


Fig. 2. Fourier transformed IR spectra of CO adsorbed on PVP-protected nanoparticles: (a) Pd, (b) Pd-core/Ag-shell (1/1), (c) Pd-core/Ag-shell (1/2), (d) Pd-core/Ag-shell (1/3), (e) Pd-core/Ag-shell (1/4), and (f) Ag nanoparticles.

separated by filtration with an ultrafilter membrane. Since the filtrates did not contain any metal ions according to qualitative analyses, we believe the yield of the bimetallic nanoparticles is almost quantitative.

Figure 1 shows the UV–vis spectra of the colloidal dispersions of polymer-protected Pd/Ag bimetallic nanoparticles at various Pd/Ag atomic ratios. The absorption peak at 380 nm can be attributed to the surface plasmon absorption of Ag nanoparticles.[26] The surface plasmon absorption of Ag cannot be observed for the colloidal dispersions of Pd/Ag bimetallic nanoparticles at a Pd/Ag atomic ratio of 1/1. This means that the Ag ions added do not form enough large Ag nanoparticles to show a plasmon absorption, but deposit on the surface of Pd nanoparticles to form only tiny spots, which are too small to show plasmon absorption. When the amount of Ag was larger than Pd, that is, the atomic ratio of Pd/Ag was less than 1/2, a strong plasmon absorption was observed. This observation suggests that the Ag atoms, produced by reduction of Ag ions with hydride on the surface of the Pd seed, cover the Pd seeds completely to form a Ag shell when the atomic ratio of Pd/Ag is less than 1/2.

Since the IR spectrum of CO adsorbed on the surface of metals varies depending on the kind of metals, FT-IR absorption spectra of carbon monoxide (CO) are often used to gain information about the surface metal.[27–29] We also used this technique. The results are shown in Fig. 2. The spectra of the seed Pd nanoparticles with adsorbed CO showed peaks at 1934 and 2044 $cm^{-1}$, while Ag nanoparticles prepared separately as a reference showed weak CO-FT-IR peaks at 1992 and 2019 $cm^{-1}$. When the Pd/Ag ratio was 1/1, the CO peaks attributed to Pd remained. When Pd/Ag = 1/2, the CO peaks due to Pd completely disappeared, while those attributed to Ag increased and shifted a little to a higher wavenumber. These results again support the formation of Pd/Ag bimetallic nanoparticles with a Pd-core/Ag-shell structure with an atomic ratio of Pd/Ag = 1/2.

Figure 3 shows the TEM images and the size distribution histograms of Pd/Ag bimetallic nanoparticles. The bimetallic nanoparticles were spherical and small, and had a considerably uniform size. The average diameter of Pd/Ag (1/2 in atomic ratio) nanoparticles was $6.8 \pm 1.8$ nm, which is larger than that of seed Pd nanoparticles ($4.4 \pm 1.2$ nm) and smaller than that of Ag nanoparticles ($10.6 \pm 1.4$ nm) that were prepared separately by glycol reduction. The average diameter of Pd/Ag

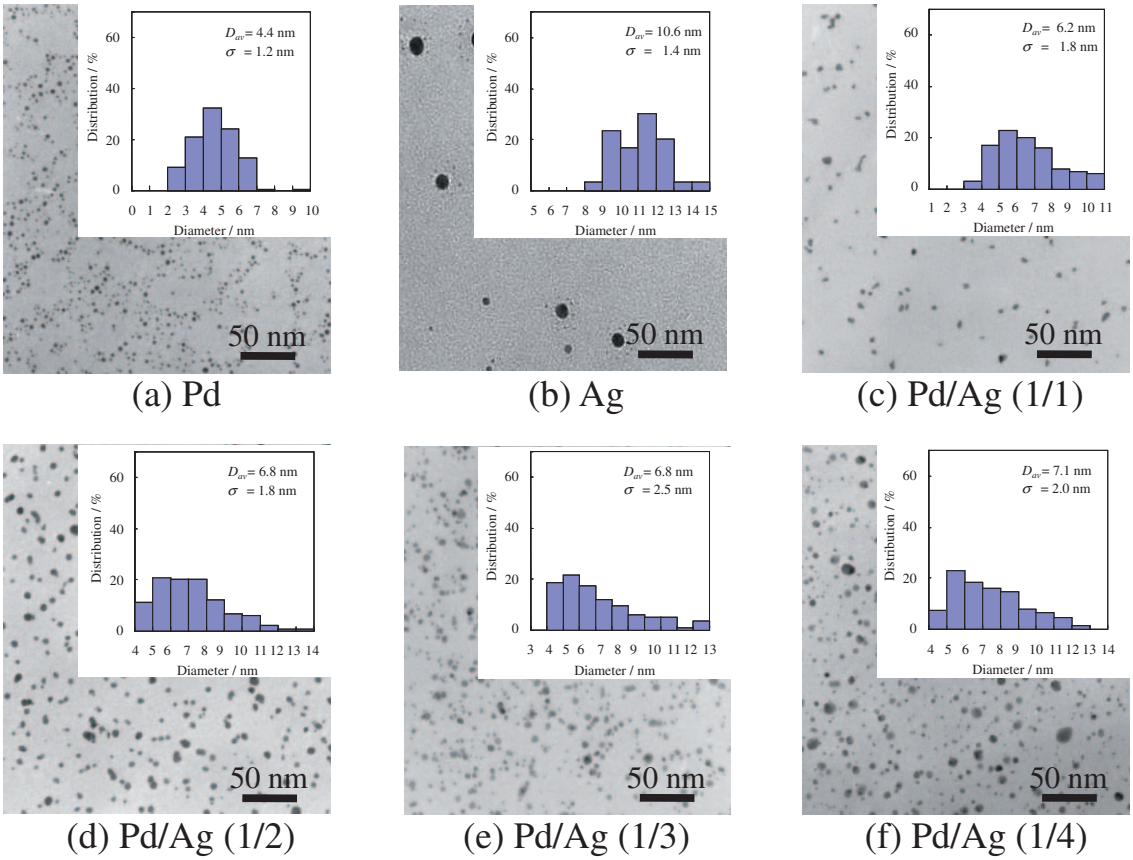


Fig. 3. TEM photographs of PVP-protected Pd and Ag monometallic, and Pd/Ag bimetallic nanoparticles: (a) Pd, (b) Ag, (c) Pd-core/Ag-shell (1/1), (d) Pd-core/Ag-shell (1/2), (e) Pd-core/Ag-shell (1/3), and (f) Pd-core/Ag-shell (1/4) nanoparticles. $D_{av}$ = average diameter, and $\sigma$ = standard deviation.

bimetallic nanoparticles increased with an increase in the Ag content in the bimetallic nanoparticles. The same tendency was observed in the case of Pd/Au[30] and Pd/Pt[20,31] bimetallic nanoparticles prepared by the same method (a sacrificial hydrogen-reduction method).

Detailed analyses of the Pd/Ag bimetallic nanoparticles were carried out using EF-TEM. Figure 4 shows the mapping of Pd and Ag in the Pd/Ag (1/2) bimetallic nanoparticles by using EELS. Green and red areas of the map show the presence of Pd and Ag, respectively. The yellow areas show the co-existence of Pd and Ag. This mapping picture clearly indicates that the Ag surrounds Pd.

Based on the results of CO-FT-IR spectra, UV–vis spectra, TEM images, and EF-TEM pictures, PVP-protected Pd/Ag (1/2) bimetallic nanoparticles prepared by a sacrificial hydrogen-reduction method are considered to have a Pd-core/Ag-shell structure.[32] This core–shell structure was also supported by comparing the catalytic activities of these nanoparticles towards the hydrogenation of methyl acrylate at 30 °C under an atmospheric pressure of hydrogen. The Pd seed had a high catalytic activity (6.71 mol-$H_2$ mol-$Pd^{-1}$ $s^{-1}$), while the Ag nanoparticles, prepared by reduction with ethylene glycol, showed almost no activity (0.049 mol-$H_2$ mol-$Ag^{-1}$ $s^{-1}$). When the atomic ratio of Pd/Ag was varied, the bimetallic nanoparticles with Pd/Ag = 1/1 had a low activity (0.115 mol-$H_2$ mol-(Pd + Ag)$^{-1}$ $s^{-1}$), while those with Pd/Ag = 1/2 had almost no activity (0.037 mol-$H_2$ mol-(Pd + Ag)$^{-1}$ $s^{-1}$), similar to the case of Ag. This result supports that, when Pd/Ag = 1/2, the Pd core is completely covered by Ag shell.

In the above-described experiments, the seed Pd nanoparticles, prepared by the reduction of palladium(II) acetate $Pd(OAc)_2$ at 160 °C in ethylene glycol in the presence of PVP at the molar ratio of monomeric residue of PVP to (Pd + Ag) (=*R*) of 40, had an average particle size of 4.4 ± 1.2 nm. The resulting Pd/Ag (1/2) bimetallic nanoparticles with a Pd-core/Ag-shell structure, prepared by sacrificial hydrogen reduction from the above Pd seeds, had an average size of 6.8 ± 1.8 nm. If we wish to prepare the smaller bimetallic nanoparticles, the seed particles should be a smaller size. For examples, the Pd seed prepared from not $Pd(OAc)_2$ but $PdCl_2$ at 160 °C in ethylene glycol had an average diameter of 2.5 ± 0.68 nm, and then the Pd/Ag (1/2) bimetallic nanoparticles prepared from this seed by a sacrificial hydrogen-reduction method had the diameter of 3.2 ± 0.73 nm. On the other hand, the Pd seeds prepared by the reduction of $PdCl_2$ in refluxing in ethylene glycol for 1 h at 198 °C had an average diameter of 1.6 ± 0.40 nm, and the Pd/Ag (1/2) bimetallic nanoparticles starting from the Pd seeds had an average diameter of 2.5 ± 0.38 nm. These three series of Pd/Ag bimetallic nanoparticles prepared by starting from three kinds of Pd seeds with different sizes showed the same tendency in the structure analyses indicating a core–shell structure and were used for preparation of trimetallic nanoparticles.

**Pd/Ag/Rh Trimetallic Nanoparticles.** As mentioned in

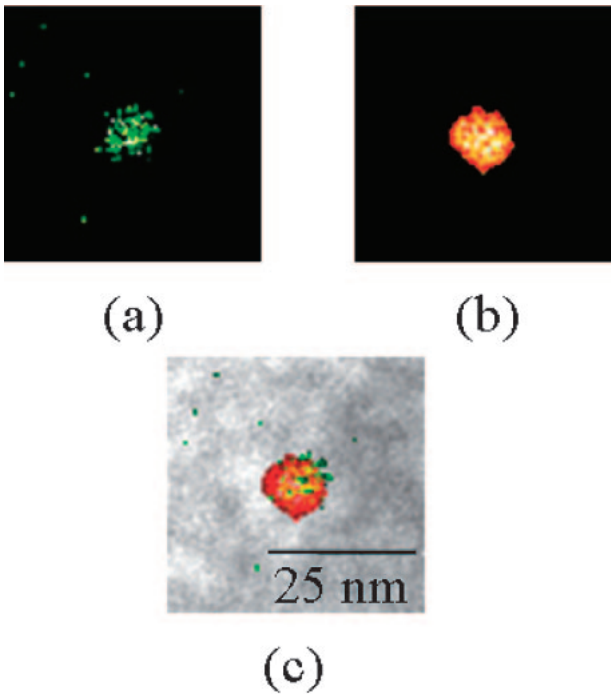


Fig. 4. EF-TEM images of Pd/Ag (1/2) bimetallic nanoparticles prepared by a sacrificial hydrogen-reduction method: (a) Pd mapping, (b) Ag mapping, and (c) total mapping of Pd and Ag (Pd, green; Ag, red; Pd + Ag, yellow).

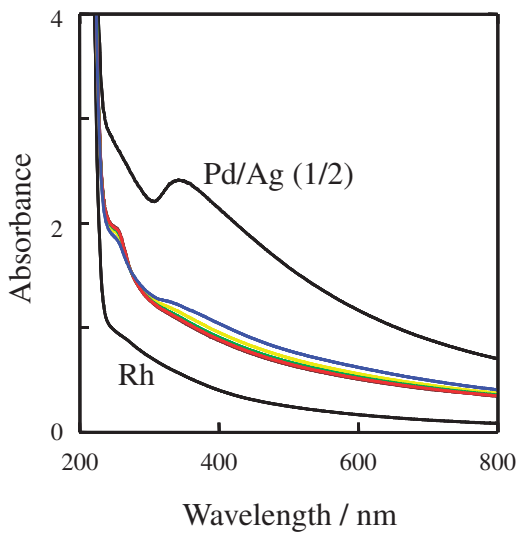


Fig. 5. UV–vis spectra of colloidal dispersions of Pd/Ag (1/2) bimetallic and Rh monometallic nanoparticles, and spectral change of the 1/1 mixtures of these two dispersions after 1 min (blue), 5 min (yellow), 10 min (green), 15 min (red), 20 min (brown) after the mixture. The original Ag surface plasmon adsorption peak of Pd/Ag bimetallic nanoparticles was quenched by keeping the mixed solution at room temperature after the addition of Rh nanoparticles.

the previous section, the colloidal dispersion of PVP-protected Pd/Ag (1/2) bimetallic nanoparticles with a Ag shell had a plasmon absorption at 380 nm. When a colloidal dispersion

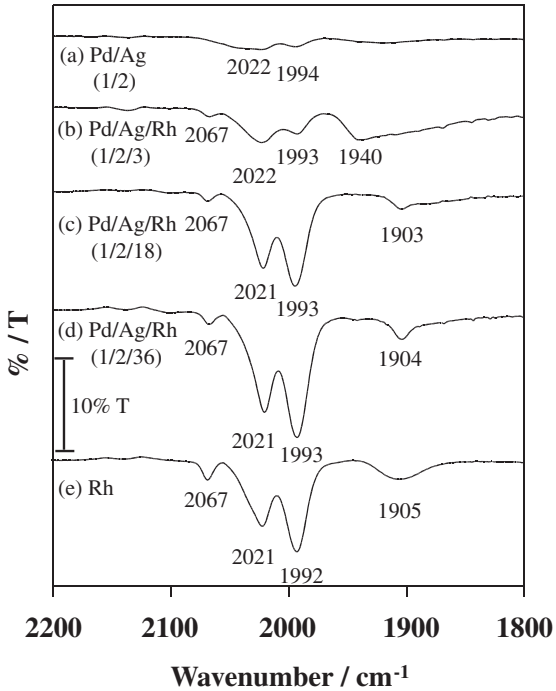


Fig. 6. Fourier transformed IR spectra of CO adsorbed on PVP-protected nanoparticles: (a) Pd-core/Ag-shell (1/2), (b) Pd-core/Ag-interlayer/Rh-shell (1/2/3), (c) Pd-core/Ag-interlayer/Rh-shell (1/2/18), (d) Pd-core/Ag-interlayer/Rh-shell (1/2/36), and (e) Rh nanoparticles.

of PVP-protected Rh nanoparticles (an average diameter = $2.5 \pm 0.83$ nm), prepared by an alcohol-reduction method, was mixed at room temperature with the colloidal dispersion of Pd/Ag (1/2) bimetallic nanoparticles (an average diameter = $6.8 \pm 1.8$ nm) prepared by a sacrificial hydrogen-reduction method, the plasmon absorption at 380 nm gradually decreased in strength and disappeared completely after 20 min, as shown in Fig. 5. This phenomenon suggests that the Ag surface of Pd/Ag bimetallic nanoparticles is covered by the Rh nanoparticles. Similar phenomena were observed in the mixture of colloidal dispersions of PVP-protected Ag nanoparticles and Rh nanoparticles, which we have previously reported.[21,22] During and after the mixing reaction of colloidal dispersions, no aggregates or precipitates were observed.

In the CO-FT-IR spectra of the mixtures of Pd/Ag (1/2) bimetallic nanoparticles and Rh nanoparticles, the peaks at 1905, 1992, 2021, and 2067 $cm^{-1}$, characteristic to Rh, rapidly increased in intensity with an increase in the amount of Rh nanoparticles added to the mixtures, as Fig. 6 shows. This observation suggests the presence of Rh on the surface of particles resulting from the mixtures.

Figure 7 shows TEM images of Rh nanoparticles and the Pd/Ag/Rh (1/2/36) trimetallic nanoparticles, produced by mixture of Pd/Ag (1/2) bimetallic nanoparticles and Rh nanoparticles at the atomic ratio of (Pd + Ag)/Rh = 1/12. The trimetallic nanoparticles were considerably uniform in size and had an average diameter of $3.5 \pm 1.3$ nm, although average diameters of Pd/Ag (1/2) and Rh nanoparticles were 6.8 and 2.5 nm, respectively. This suggests that the particles produced by the mixture are not composed of two independent kinds of

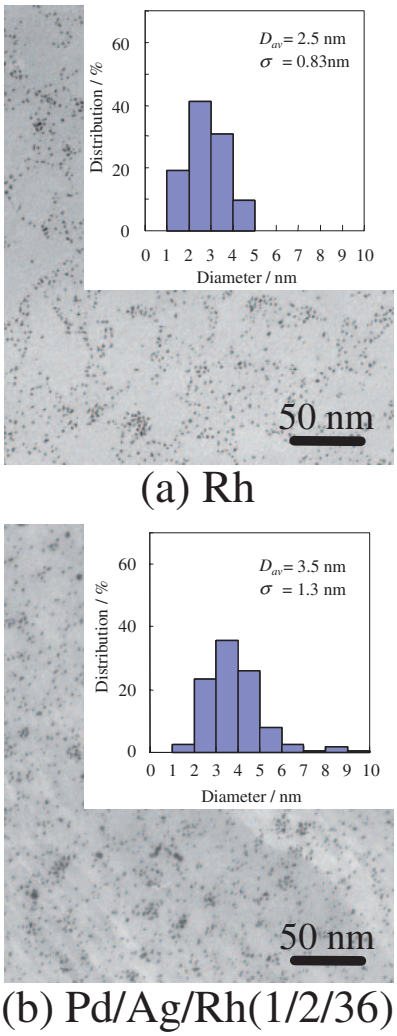


Fig. 7. TEM photographs of PVP-protected (a) Rh monometallic, and (b) Pd/Ag/Rh (1/2/36) trimetallic nanoparticles: $D_{av}$ = average diameter, $\sigma$ = standard deviation.

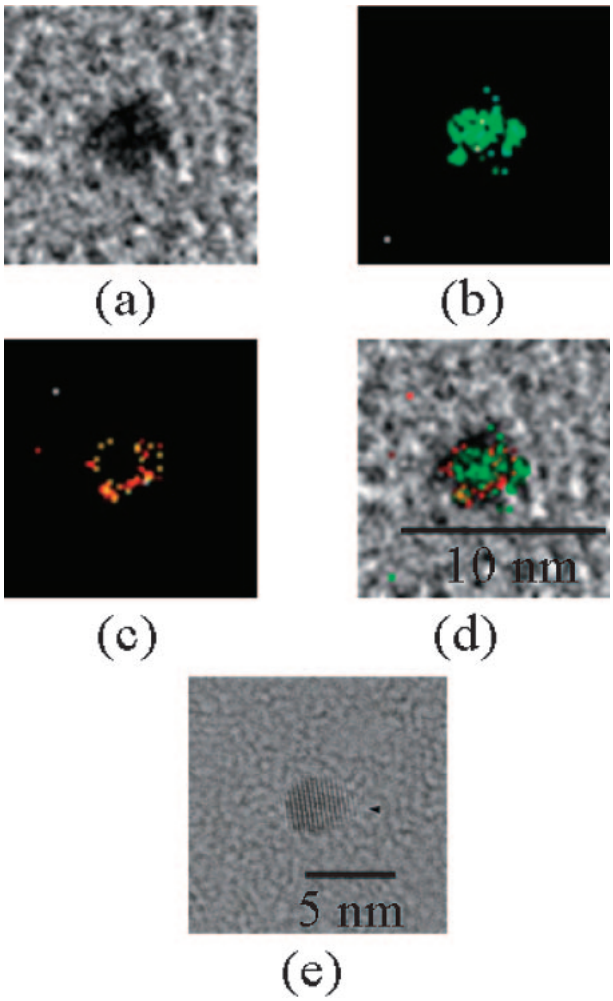


Fig. 8. EF-TEM images and HR-TEM photograph of Pd/Ag/Rh (1/2/36) trimetallic nanoparticles: (a) Zeroloss image, (b) Ag mapping, (c) Rh mapping, (d) total mapping of Ag and Rh (Ag, green; Rh, red; Ag + Rh, yellow), and (e) HR-TEM photograph.

particles, but of alloyed trimetallic nanoparticles. The HR-TEM image and EF-TEM mapping are shown in Fig. 8. EF-TEM mapping showed that Rh atoms were located not in the center of the particles, but rather on the surface of the particles. The HR-TEM image showed that the particles were the mostly single crystals and were composed of three elements on the basis of EDS spectra, although some polycrystalline structures were also observed. Since all of the bulk crystals of Pd, Ag, and Rh have a face-centered cubic structure, in the Pd/Ag/Rh trimetallic nanoparticles the Ag interlayer can grow epitaxially on the Pd seed, and the Rh shell also can grow up epitaxially on the Ag interlayer, resulting in almost single crystal structure.[33–35]

Although we have no strict evidence on the structure of the present PVP-protected Pd/Ag/Rh (1/2/36) trimetallic nanoparticles, the above CO-FT-IR, TEM, HR-TEM, and EF-TEM results suggest the spontaneous formation of a triple core–shell structure or a Pd-core/Ag-interlayer/Rh-shell structure by self-organization. This structure is also supported by the high catalytic activity of these trimetallic nanoparticles, described in the next section.

**Catalytic Activity of Trimetallic Nanoparticles.** PVP-protected Pd/Ag/Rh trimetallic nanoparticles at various atomic ratios of (Pd + Ag)/Rh were prepared by self-organization starting from Pd/Ag (1/2) bimetallic nanoparticles and Rh nanoparticles. Here, we used Pd/Ag bimetallic nanoparticles only at the atomic ratio of 1/2, because the Pd seed core is completely covered by Ag at an atomic ratio of 1/2, as described in the previous section. These trimetallic nanoparticles with various atomic ratios were used as catalysts for hydrogenation of methyl acrylate at 30 °C under an atmosphere of hydrogen. The catalytic activity was calculated by dividing the initial rate of hydrogen uptake per second with total amount of used metals (Pd + Ag + Rh). The catalytic activity varied with the composition of trimetallic nanoparticles. In the series of trimetallic nanoparticles prepared from Pd/Ag (1/2) bimetallic nanoparticles (average diameter = 6.8 ± 1.8 nm) and Rh nanoparticles (average diameter = 2.5 ± 0.83 nm), the catalytic activity varied an increase in the atomic ratio of Rh to (Pd + Ag) as shown in Fig. 9. In other words, the highest catalytic activity was achieved by the trimetallic nanoparticles at the

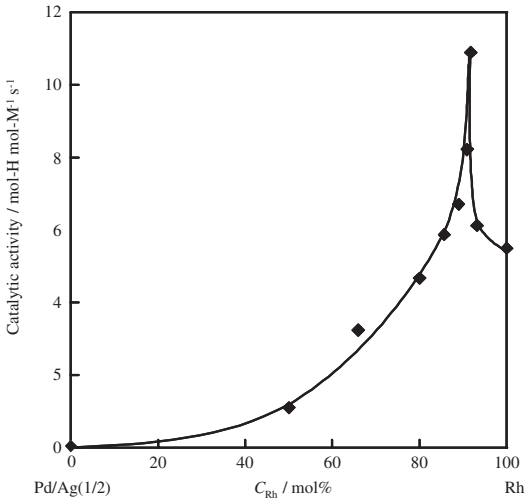


Fig. 9. Relationship between metal composition and catalytic activity of PVP-protected Pd/Ag/Rh trimetallic nanoparticles for hydrogenation of methyl acrylate. The trimetallic nanoparticles were prepared by starting from Pd/Ag (1/2) bimetallic nanoparticles (av. diameter = 6.8 nm) and Rh nanoparticles (av. diameter = 2.5 nm). The concentration of Rh $C_{Rh}$ shows the % atomic ratio of Rh in total metal (Pd + Ag + Rh).

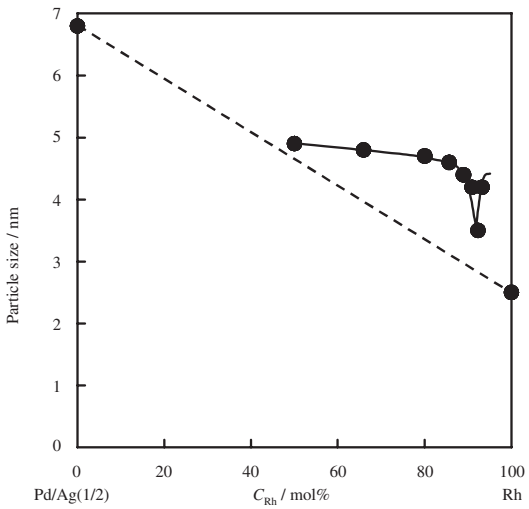


Fig. 10. Average diameter of PVP-protected Pd/Ag/Rh trimetallic nanoparticles as a function of Rh content. The trimetallic nanoparticles are the same as those used for measurements of catalytic activities shown in Fig. 9. The dashed line indicates average particles sizes estimated for the mixtures without any reaction.

atomic ratio of 1/2/36. Interestingly the catalytic activity had a sharp maximum peak at this point, where the average diameter was the smallest (3.5 ± 1.3 nm) among a series of trimetallic nanoparticles starting from the Pd/Ag (1/2) bimetallic nanoparticles (6.8 ± 1.8 nm) and Rh nanoparticles (2.5 ± 0.83 nm) (cf. Fig. 10). Even when the catalytic activity was normalized by dividing the activity with total surface area of the catalyst, the same tendency was observed. Thus, the atomic ratio of 1/2/36 (Pd/Ag/Rh) could be a magic ratio for the present system and could be determined naturally during the self-

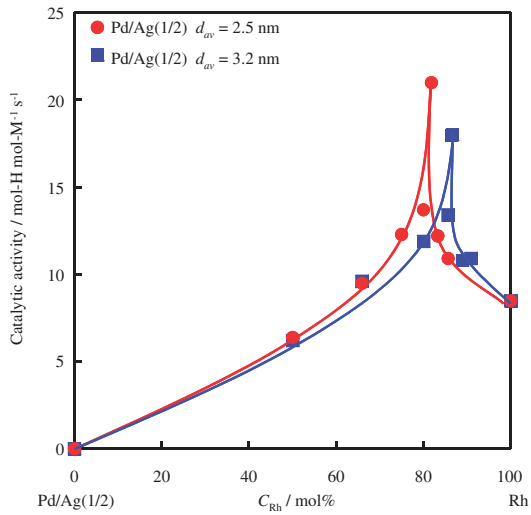


Fig. 11. The relationship between metal composition and catalytic activity of PVP-protected Pd/Ag/Rh trimetallic nanoparticles for hydrogenation of methyl acrylate. The trimetallic nanoparticles were prepared by starting from Pd/Ag (1/2) bimetallic nanoparticles with average diameters of ● 2.5 ± 0.38 nm, and ■ 3.2 ± 0.73 nm. The concentration of Rh $C_{Rh}$ shows the % atomic ratio of Rh in total metal (Pd + Ag + Rh).

organization process. Note that these results are reproduced.

When the Pd/Ag (1/2) bimetallic nanoparticles with the smaller sizes than this case, i.e., those of an average diameter of 3.2 ± 0.73 and 2.5 ± 0.38 nm, were used instead of those of 6.8 ± 1.8 nm, the dependence of catalytic activity on the metal composition varied as shown in Fig. 11. The highest catalytic activities were observed for atomic ratios of 1/2/21 (Pd/Ag/Rh) and 1/2/13.5, and the average diameters of trimetallic nanoparticles at these composition were 2.6 ± 0.58 nm and 2.2 ± 0.59 nm, respectively. These two kinds of Pd/Ag/Rh trimetallic nanoparticles showed the same tendency in structure analyses as those of trimetallic nanoparticles prepared from Pd/Ag (1/2) bimetallic nanoparticles (average diameter = 6.8 ± 1.8 nm) and Rh nanoparticles. Again, the trimetallic nanoparticles with highest catalytic activity had the smallest average diameter. The high catalytic activity, however, is not due to a large surface area. In fact, even if the activity is normalized to the surface area, the trimetallic nanoparticles with the smallest size still have the highest catalytic activity.

The average diameter of the last trimetallic nanoparticles was smaller than those of both starting materials, that is, Pd/Ag (1/2) bimetallic and Rh nanoparticles. This phenomenon is very interesting, if the successive deposition mechanism, which is a commonly accepted mechanism, is assumed. Thus, any kind of re-alignment should occur during the self-organization process. A similar consideration has been also discussed in the case of self-organization between Ag and Rh nanoparticles.[21,22,25] The catalytic activity of Pd/Ag/Rh trimetallic nanoparticles with a triple core–shell, i.e., a Pd-core/Ag-interlayer/Rh-shell structure prepared by self-organization, was compared to those of the corresponding monometallic and bimetallic nanoparticles as well as trimetallic nanoparticles prepared by other methods. The results are shown in Fig. 12.

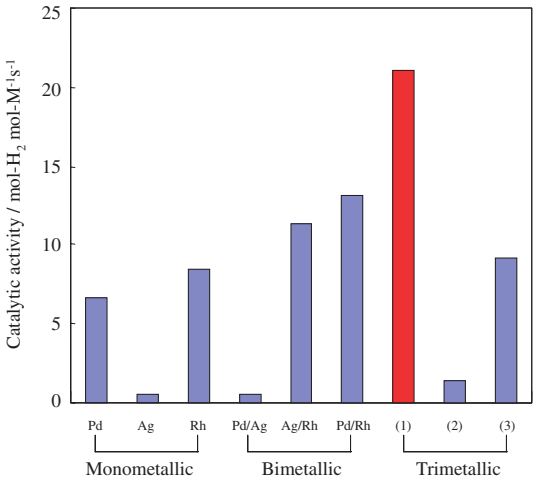


Fig. 12. Catalytic activity of Pd, Ag, and Rh monometallic nanoparticles, Pd/Ag (1/2), Ag/Rh (1/4), and Pd/Rh (1/2) bimetallic nanoparticles, and Pd/Ag/Rh (1/2/13.5) trimetallic nanoparticles: (1) The trimetallic nanoparticles prepared by self-organization starting from Pd/Ag (1/2) bimetallic and Rh nanoparticles, (2) those prepared by simultaneous reduction, and (3) those prepared by self-organization by mixing of Pd, Ag, and Rh monometallic nanoparticles. The atomic composition Pd/Ag/Rh was kept constant 1/2/13.5 for all trimetallic nanoparticles. See the text for details of preparation of monometallic and bimetallic nanoparticles.

In Fig. 12, the catalytic activities of monometallic and bimetallic nanoparticles are shown for comparison. The colloidal dispersions of PVP-protected Pd, Ag, and Rh monometallic nanoparticles used for these measurements were prepared by an alcohol-reduction method in ethanol/water. The catalytic activity of Pd/Ag (1/2) bimetallic nanoparticles with a Pd-core/Ag-shell structure is also shown in Fig. 12 for comparison. In the case of other bimetallic nanoparticles, various kinds of reference nanoparticles were prepared with different atomic ratios by two methods, i.e., simultaneous reduction and physical mixing (self-organization). The highest activities for Ag/Rh (1/4) by physical mixing and Pd/Rh (1/2) bimetallic nanoparticles by simultaneous reduction are shown in Fig. 12.

In the series of the Pd/Ag/Rh trimetallic nanoparticles prepared by mixing three kinds of Pd/Ag (1/2) bimetallic nanoparticles with Rh nanoparticles, the Pd/Ag/Rh (1/2/13.5) nanoparticles with an average diameter of $2.2 \pm 0.59$ nm had the highest catalytic activity (21.0 mol-$H_2$ mol-$M^{-1}$ $s^{-1}$), while the Pd/Ag/Rh (1/2/36) nanoparticles with an average diameter of $3.5 \pm 1.3$ nm and Pd/Ag/Rh (1/2/21) nanoparticles with an average diameter of $2.6 \pm 0.58$ nm had activites of 11.0 and 18.0 mol-$H_2$ mol-$M^{-1}$ $s^{-1}$, respectively. Thus, the smaller the particle size is the higher the catalytic activity. This result is not due to the surface area. In fact, when the activity was normalized to the surface area, the trimetallic nanoparticles with the smallest size still had the highest catalytic activity.

Now, the catalytic activity of Pd/Ag/Rh (1/2/13.5) nanoparticles prepared by self-organization was compared to those of trimetallic nanoparticles prepared by other methods. At first, the simultaneous reduction method was used for preparation of trimetallic nanoparticles. Thus, a 1/9 (v/v) water/ethanol solution of $Pd(OAc)_2$, $AgClO_4$, and $Rh(NO_3)_3$ with a molar ratio of 1/2/13.5 was refluxed for 3 h under nitrogen. The obtained trimetallic nanoparticles had an average diameter of $2.5 \pm 0.69$ nm. This was thought to be small enough for the particles to show a high catalytic activity, but the catalytic activity was, in fact, very small (0.59 mol-$H_2$ mol-$M^{-1}$ $s^{-1}$). This is probably due to the structure of trimetallic nanoparticles prepared by simultaneous reduction, which may provide the structure different from Pd-core/Ag-interlayer/Rh-shell, like Pd-core/Rh-interlayer/Ag-shell. This structure is based on the formation mechanism proposed for simultaneous reduction[23] and is supported by the appearance of a plasmon resonance peak at 350 nm in the colloidal dispersion of these trimetallic nanoparticles.

The other preparation method was self-organization among the Pd, Ag, and Rh monometallic nanoparticles with average diameters of 2.3, 5.3, and 2.5 nm, respectively. PVP-protected Pd, Ag, and Rh nanoparticles separately prepared by alcohol reduction were mixed at room temperature, and the mixtures were kept at room temperature for 3 days. The resulting mixture had a wide size distribution with an average diameter of $3.3 \pm 3.7$ nm, and no plasmon absorption was observed. This suggests that the colloidal dispersions, prepared by self-organization, might be a mixture of Ag-core/Pd-shell and Ag-core/Rh-shell bimetallic nanoparticles, or alloyed bimetallic and/or trimetallic nanoparticles. In fact, the trimetallic nanoparticles had a reasonably high catalytic activity (9.2 mol-$H_2$ mol-$M^{-1}$ $s^{-1}$). This catalytic activity data is roughly consistent with the structure speculated above. We also tried to synthesize PVP-protected Pd/Ag/Rh trimetallic nanoparticles using Pd/Ag bimetallic nanoparticles prepared by simultaneous reduction. However, the trimetallic nanoparticles with a triple core/shell structure could not be prepared by this method.[36]

Based on the comparison among the catalytic activities of trimetallic nanoparticles shown in Fig. 12, the Pd/Ag/Rh (1/2/13.5) nanoparticles prepared by the self-organization from Pd-core/Ag-shell (1/2) bimetallic nanoparticles (average diameter $= 2.5 \pm 0.38$ nm) and Rh nanoparticles had the highest catalytic activity. This can be understood by the successive electronic charge transfer from Rh-shell to Ag-interlayer and Ag-interlayer to Pd-core in triple core–shell-structured trimetallic nanoparticles.[23,25] Other trimetallic nanoparticles did not have such an ideal structure for successive electronic effect, which could be the reason why the other trimetallic nanoparticles had lower activity.

## Conclusion

Colloidal dispersions of PVP-protected Pd/Ag bimetallic nanoparticles with a Pd-core/Ag-shell structure were prepared by a sacrificial hydrogen-reduction method starting from colloidal dispersions of PVP-protected Pd seed nanoparticles. The core–shell structures were supported by UV–vis absorption and CO-FT-IR spectroscopes, TEM, and EF-TEM. When the atomic ratio of Pd/Ag was 1/2, the Pd seed cores were considered to be completely covered by Ag layers.

The physical mixture of colloidal dispersions of PVP-protected Pd/Ag (1/2) bimetallic nanoparticles and Rh nanoparticles at room temperature resulted in the formation of colloi-

dal dispersions of Pd/Ag/Rh trimetallic nanoparticles by self-organization. The trimetallic nanoparticles, thus prepared, appeared to have a triple core–shell structure, i.e., a Pd-core/Ag-interlayer/Rh-shell structure, by UV–vis absorption spectra, FT-IR spectra of adsorbed CO, TEM, HR-TEM, and EF-TEM.

The catalytic activities of the PVP-protected Pd/Ag/Rh trimetallic nanoparticles were measured by the rate of hydrogen uptake during hydrogenation of methyl acrylate in ethanol/water at 30 °C under an atmosphere of hydrogen and compared with those of monometallic and bimetallic nanoparticles and trimetallic nanoparticles prepared by other methods. The Pd/Ag/Rh trimetallic nanoparticles, prepared by self-organization starting from the smallest Pd/Ag (1/2) bimetallic nanoparticles with an average diameter $2.5 \pm 0.38$ nm and having an atomic composition of Pd/Ag/Rh = 1/2/13.5, had the smallest average diameter ($2.2 \pm 0.59$ nm) among the trimetallic nanoparticles tested here and had the highest catalytic activity for the hydrogenation of an olefin among the metal nanoparticles tested here.

The high catalytic activity of the Pd/Ag/Rh (1/2/13.5) trimetallic nanoparticles, having a Pd-core/Ag-interlayer/Rh-shell structure, is considered to be due to successive electron transfer between the metals in a particle, i.e., Rh-shell to Ag-interlayer and Ag-interlayer to Pd-core. Thus, it is suggested that the concept of the successive or sequential electron transfer, which is known to be very important in living organisms, like the photosynthetic system, is also useful for the design of new multi-metallic catalysts.

This work was supported by a Grant-in-Aid for Scientific Research (B) (No. 15310078) by the Ministry of Education, Culture, Sports, Science and Technology (MEXT), Japan.

## Supporting Information

X-ray diffraction patterns of PVP-protected Pd, Ag, and Rh monometallic, Pd/Ag bimetallic nanoparticles, and Pd/Ag/Rh trimetallic nanoparticles (Fig. S1), catalytic activity normalized by surface area as a function of metal composition of PVP-protected Pd/Ag/Rh trimetallic nanoparticles for hydrogenation of methyl acrylate (Fig. S2) and comparison of normalized catalytic activity of monometallic, bimetallic, and trimetallic nanoparticles (Fig. S3) are shown in Supporting Information. This material is available free of charge on the web at http://www.csj.jp/journals/bcsj/.

## References

1 H. Bönnemann, R. M. Richards, *Eur. J. Inorg. Chem.* **2001**, 2455.

2 *Clusters and Colloids from Theory to Application*, ed. by G. Schmid, VCH, Weinheim, **1994**.

3 H. Hirai, N. Toshima, *Tailored Metal Catalyst*, ed. by Y. Iwasawa, Reidel, Dordrecht, **1985**, pp. 121–135.

4 H. Bönnemann, W. Brijoux, R. Brinkmann, E. Dinjus, T. Jouben, B. Korall, *Angew. Chem., Int. Ed. Engl.* **1991**, *30*, 1312.

5 C. Amiens, D. de Caro, B. Chaudret, J. S. Bradley, R. Mazel, C. Roucau, *J. Am. Chem. Soc.* **1993**, *115*, 11638.

6 N. Toshima, Y. Shiraishi, T. Teranishi, M. Miyake, T. Tominaga, H. Watanabe, W. Brijoux, H. Bönnemann, G. Schmid, *Appl. Organomet. Chem.* **2001**, *15*, 178.

7 H. Tsunoyama, H. Sakurai, Y. Negishi, T. Tsukuda, *J. Am. Chem. Soc.* **2005**, *127*, 9374.

8 S. Sun, C. B. Murray, D. Weller, L. Folk, A. Moser, *Science* **2000**, *287*, 1989.

9 M. Chen, J. Kim, J. P. Liu, H. Fan, S. Sun, *J. Am. Chem. Soc.* **2006**, *128*, 7132.

10 M. Nakaya, M. Kanehara, T. Teranishi, *Langmuir* **2006**, *22*, 3485.

11 X. Du, N. Toshima, *Chem. Lett.* **2006**, *35*, 1254.

12 T. Teranishi, M. Nishida, M. Kanehara, *Chem. Lett.* **2005**, *34*, 1004.

13 a) N. Watanabe, J. Kawamata, N. Toshima, *Chem. Lett.* **2004**, *33*, 1368. b) N. Watanabe, N. Toshima, *Bull. Chem. Soc. Jpn.* **2007**, *80*, 208.

14 S. Kobayashi, T. Miyama, N. Nishida, Y. Sakai, H. Shiraki, Y. Shiraishi, N. Toshima, *J. Disp. Technol.* **2006**, *2*, 121.

15 Y. Shiraishi, N. Toshima, K. Maeda, H. Yoshikawa, J. Xu, S. Kobayashi, *Appl. Phys. Lett.* **2002**, *81*, 2845.

16 H. Iida, T. Nakanishi, T. Osaka, *Electrochim. Acta* **2005**, *51*, 855.

17 N. Toshima, M. Harada, T. Yonezawa, K. Kushihashi, K. Asakura, *J. Phys. Chem.* **1991**, *95*, 7448.

18 N. Toshima, M. Harada, Y. Yamazaki, K. Asakura, *J. Phys. Chem.* **1992**, *96*, 9927.

19 N. Toshima, Y. Wang, *Langmuir* **1994**, *10*, 4574.

20 Y. Wang, N. Toshima, *J. Phys. Chem. B* **1997**, *101*, 5301.

21 K. Hirakawa, N. Toshima, *Chem. Lett.* **2003**, *32*, 78.

22 N. Toshima, M. Kanemaru, Y. Shiraishi, Y. Koga, *J. Phys. Chem. B* **2005**, *109*, 16326.

23 N. Toshima, T. Yonezawa, *New J. Chem.* **1998**, *22*, 1179.

24 A. Henglein, *J. Phys. Chem. B* **2000**, *104*, 6683.

25 N. Toshima, Y. Shiraishi, T. Matsushita, H. Mukai, K. Hirakawa, *Int. J. Nanosci.* **2002**, *1*, 397.

26 Y. Shiraishi, N. Toshima, *Colloids Surf., A* **2000**, *169*, 59.

27 M. R. Mucalo, R. P. Cooney, *J. Chem. Soc., Faraday Trans.* **1991**, *87*, 1221.

28 L. N. Lewis, N. Lewis, *J. Am. Chem. Soc.* **1986**, *108*, 7228.

29 J. S. Bradley, G. H. Via, L. Bonnevio, E. W. Hill, *Chem. Mater.* **1996**, *8*, 1895.

30 Y. Shiraishi, D. Ikenaga, N. Toshima, *Aust. J. Chem.* **2003**, *56*, 1025.

31 N. Toshima, Y. Shiraishi, A. Shiotsuki, D. Ikenaga, Y. Wang, *Eur. Phys. J. D* **2001**, *16*, 209.

32 The XRD pattern of Pd/Ag (1/2) bimetallic nanoparticles, Fig. S1 in Supporting Information, showed that the peak position of the bimetallic nanoparticles was near that of the Pd nanoparticles but was shifted a little towards the position of Ag nanoparticles, suggesting the epitaxial growth of the Ag shell on the Pd seed.[33,34]

33 C. Ricolleau, L. Audinet, M. Gandais, T. Gacoin, *Thin Solid Films* **1998**, *336*, 213.

34 J. H. Hodak, A. Henglein, M. Giersig, G. V. Hartland, *J. Phys. Chem. B* **2000**, *104*, 11708.

35 In XRD of Pd/Ag/Rh trimetallic nanoparticles, the position was similar to that of Rh nanoparticles, because the trimetallic nanoparticles are mainly composed of Rh.

36 The PVP-protected Pd/Ag/Rh trimetallic starting from the Pd/Ag bimetallic nanoparticles that were prepared by sacrificial hydrogen reduction have higher catalytic activity than those starting from the Pd/Ag bimetallic nanoparticles by simultaneous reduction.